

# Optimal Modeling Parameters for Higher Order MoM-SIE and FEM-MoM Electromagnetic Simulations

Eve M. Klopf, *Student Member, IEEE*, Nada J. Šekeljić, *Student Member, IEEE*, Milan M. Ilić, *Member, IEEE*, and Branislav M. Notaroš, *Senior Member, IEEE*

**Abstract**—General guidelines and quantitative recipes for adoptions of optimal higher order parameters for computational electromagnetics (CEM) modeling using the method of moments and the finite element method are established and validated, based on an exhaustive series of numerical experiments and comprehensive case studies on higher order hierarchical CEM models of metallic and dielectric scatterers. The modeling parameters considered are: electrical dimensions of elements (*h*-refinement), polynomial orders of basis functions (*p*-refinement), orders of Gauss-Legendre integration formulas (integration accuracy), and geometrical (curvature) orders of elements in the model. The goal of the study, which is the first such study of higher order parameters in CEM, is to reduce the dilemmas and uncertainties associated with the great modeling flexibility of higher order elements, basis and testing functions, and integration procedures (this flexibility is the principal advantage but also the greatest shortcoming of the higher order CEM), and to ease and facilitate the decisions to be made on how to actually use them, by both CEM developers and practitioners.

**Index Terms**—Curved parametric elements, electromagnetic analysis, finite element method, higher order modeling, hybrid methods, integral-equation techniques, method of moments, polynomial basis functions, radar cross section, scattering.

## I. INTRODUCTION

RELATIVELY recently the computational electromagnetics (CEM) community has started to very extensively investigate and employ higher order surface and volume elements for geometrical modeling of electromagnetic structures and higher order basis functions for the approximation of currents and/or fields within the elements, mostly in the frame of the method of moments (MoM), the finite element method (FEM), and hybrid approaches [1]–[12]. However, the prin-

cipal advantage of higher order (also known as large-domain or entire-domain) techniques, their flexibility in terms of the size and shape of elements and spans of approximation functions, which can greatly reduce the number of unknowns for a given problem and enhance the accuracy and efficiency of the CEM analysis, is also their greatest shortcoming—in terms of dilemmas, uncertainties, and so many open, equally attractive, options and decisions to be made on how to actually use them. In other words, the additional flexibility can be also considered a drawback in a sense that a user has to handle many more parameters in building an EM model, which requires much deeper knowledge and understanding of the technique, and a great deal of modeling experience and expertise, and possibly considerably increases the overall simulation (modeling plus computation) time.

In terms of previous research toward the development of general guidelines and quantitative recipes for adoptions of higher order parameters for CEM modeling, a 1970 paper [13] shows that the current along a thin straight wire dipole that is a wavelength ( $\lambda$ ) long can be accurately calculated using MoM with entire-domain polynomial basis functions of the fourth order along each of the dipole arms. In [14] and [15], it has been shown that with polynomial basis functions as few as only three to four unknowns per  $\lambda$  suffice for an accurate MoM analysis of wires. In an entire-domain MoM analysis of a  $\lambda \times \lambda$  large metallic plate scatterer [16], polynomial orders of 6 to 9 yield almost identical solutions for the surface currents, with an eighth-order solution being adopted as a benchmark. Polynomial approximation of the eighth order provides an optimal solution for the volume current distribution in the MoM analysis of a  $2\lambda$  long rod-like dielectric scatterer [17]. A large-domain 1-D FEM numerical study [18] demonstrates that the optimal order of 1-D polynomial elements is about seven in single precision, with five unknowns per  $\lambda$ . Works on a higher order MoM in the framework of the surface integral equation (SIE) approach, FEM, and hybrid FEM-MoM techniques [7], [10]–[12] demonstrate examples using 2-D and 3-D elements that are about  $2\lambda$  in each dimension.

In addition, an excellent and extremely comprehensive mathematical survey of integration formulas, relevant for MoM and FEM computations, can be found in [19]. In CEM, moreover, the accuracy and efficiency of numerical integrations are tightly coupled to singularity cancellation and extraction techniques [1], [17], [20], [21]. However, as we deal in this study with elements of various electrical sizes (up to very large ones), we seek

Manuscript received July 23, 2011; revised October 15, 2011; accepted November 15, 2011. Date of publication April 18, 2012; date of current version May 29, 2012. This work was supported by the National Science Foundation under Grants ECCS-0650719 and ECCS-1002385 and in part by the Serbian Ministry of Science and Technological Development under Grant TR-32005.

E. M. Klopf, N. J. Šekeljić, and B. M. Notaroš are with Colorado State University, Department of Electrical and Computer Engineering, Fort Collins, CO 80523-1373 USA (e-mail: klopf@engr.colostate.edu; inadasek@engr.colostate.edu; notaros@colostate.edu).

M. M. Ilić is with University of Belgrade, School of Electrical Engineering, 11120 Belgrade, Serbia. He is also with the Colorado State University, Department of Electrical and Computer Engineering, Fort Collins, CO 80523-1373 USA (e-mail: milanilic@etf.rs).

Color versions of one or more of the figures in this paper are available online at <http://ieeexplore.ieee.org>.

Digital Object Identifier 10.1109/TAP.2012.2194669

rules and guidelines that would relate the number of integration points ( $N_{\text{integration}}$ ) to the order of basis functions ( $N_{\text{basis}}$ ) in each direction in the element. In [17], the formula  $N_{\text{integration}} = N_{\text{basis}} + 1$  in the context of the Gauss-Legendre quadrature is found to be an optimal choice in a higher order MoM solution to a volume integral equation, and the same formula is used in [3], where it is also reported that the minimal number of integration points, needed by the Galerkin method, often approaches the number of unknowns. In the low-order FEM technique [22], a constant five-point Gauss-Legendre formula is utilized. In the higher order FEM technique [10], the Gauss-Legendre integration formula in  $N_{\text{integration}} = N_{\text{basis}} + 10$  points is implemented. In [23],  $2(p + 1) + 1$  Gaussian points, where  $p$  is the element order, are employed in each direction for the semi-analytical integration scheme in an electromagnetic scattering code. Finally, in the higher order MoM technique with Lagrange-type interpolatory polynomial basis functions [6], a 12-point Gaussian quadrature is used for the third-order basis functions on curvilinear triangles, as it is found that such a quadrature yields a well-conditioned matrix.

This paper develops—through very extensive numerical experiments and studies using higher order MoM-SIE and hybrid FEM-MoM techniques [7], [12]—as precise as possible quantitative recipes for adoptions of optimal (or nearly optimal) higher order and large-domain parameters for electromagnetic modeling. The parameters considered are: the number of elements or electrical dimensions of elements (subdivisions) in the model ( $h$ -refinement), polynomial orders of basis functions ( $p$ -refinement), which are the same as the orders of testing functions (we use the Galerkin method for testing), orders of Gauss-Legendre integration formulas (numbers of integration points—integration accuracy), and geometrical orders of elements (orders of Lagrange-type curvature) in the model. All these parameters can, theoretically, be arbitrary. By optimal parameters we mean the values of parameters that ideally (for simple problems) yield an accurate solution employing the least possible computational resources, or (for complex problems) provide a firm initial model (starting point) that can be further refined in a straightforward fashion, and the results can be checked for convergence. This is the first such study of higher order parameters in CEM (some preliminary results of the study are presented in [24]). The ultimate goal of this work and the continued future work in this area is to reduce those dilemmas and uncertainties associated with the great modeling flexibility of higher order elements and basis and testing functions, and to ease and facilitate their use, by both CEM developers and practitioners.

Section II of the paper briefly presents the main numerical components of the higher order MoM-SIE and hybrid FEM-MoM techniques and defines all modeling parameters that are to be studied. Section III proposes and discusses a systematic analysis procedure and strategy for determining optimal parameters through numerical experiments. In Section IV, an exhaustive series of simulations and comprehensive case studies on higher order models of metallic and dielectric scatterers is performed, through which a set of general guidelines and instructions and quantitative recipes for adoptions of optimal simulation parameters is established and validated. Section V summarizes the main conclusions of the study, and

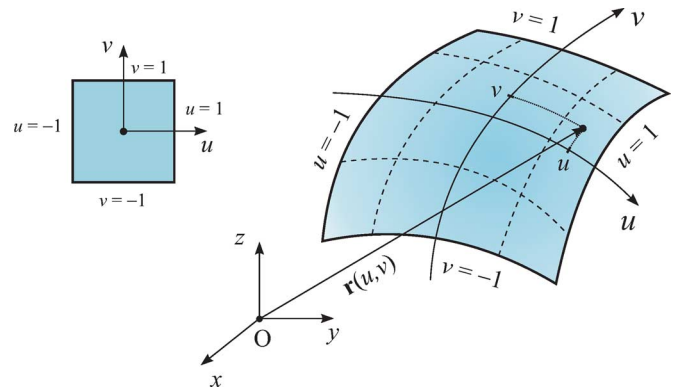


Fig. 1. Generalized curved parametric quadrilateral, with the square parent domain.

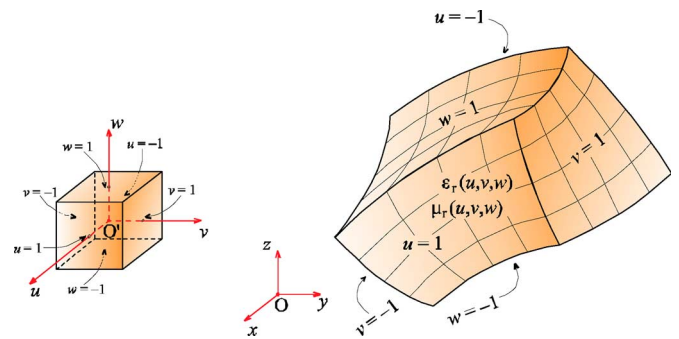


Fig. 2. Generalized curved parametric hexahedron; cubical parent domain is also shown.

puts them in a broader perspective of current and future CEM research and practice.

## II. MODELING PARAMETERS IN HIGHER ORDER MOM-SIE AND HYBRID FEM-MoM TECHNIQUES

In MoM-SIE and FEM-MoM techniques, metallic and dielectric surfaces of an electromagnetic structure (antenna or scatterer) under consideration are modeled using Lagrange-type generalized curved parametric quadrilaterals of arbitrary geometrical orders  $K_u$  and  $K_v$  ( $K_u, K_v \geq 1$ ) [7], shown in Fig. 1. Electric and magnetic surface current density vectors,  $\mathbf{J}_s$  and  $\mathbf{M}_s$ , over every generalized quadrilateral in the model are approximated by means of divergence-conforming hierarchical-type polynomial vector basis functions in parametric coordinates  $u$  and  $v$ , with arbitrary current-expansion orders  $N_u$  and  $N_v$  ( $N_u, N_v \geq 1$ ) [7], which are entirely independent from the element geometrical orders ( $K_u$  and  $K_v$ ).

The building block for volumetric FEM modeling is a Lagrange-type interpolation generalized hexahedron, in Fig. 2, with geometrical orders  $K_u$ ,  $K_v$ , and  $K_w$  ( $K_u, K_v, K_w \geq 1$ ) [10]–[12]. The electric field vector,  $\mathbf{E}$ , inside FEM hexahedra is approximated by curl-conforming hierarchical polynomial vector expansions of orders  $N_u$ ,  $N_v$ , and  $N_w$  ( $N_u, N_v, N_w \geq 1$ ) [10].

In both MoM-SIE and FEM-MoM techniques, the equations are tested by means of the Galerkin method, i.e., using the same functions used for current expansion. The resulting generalized Galerkin impedances (the system matrix elements)

corresponding to testing functions defined on the  $m$ th quadrilateral patch and basis functions defined on the  $n$ th patch in the model (or to different testing and basis function sets on the same patch), for one of the homogeneous material domains in the structure, can be found as linear combinations of basic Galerkin potential and scalar field integrals  $\xi$  and  $\zeta$  given in [7]. When the source-to-field distance  $R = |\mathbf{r}_m - \mathbf{r}_n|$  in Green's function ( $g$ ) is zero or small, the procedure of extracting the (quasi)singularity in integrals is performed [17]. A typical FEM-FEM Galerkin matrix entry contains a volumetric (three-fold) integral over a generalized hexahedron (Fig. 2) in the model [10]. The numerical integration is carried out using the Gauss-Legendre integration formula. For example, the four-fold integration formula for the quadruple integrals  $\xi$  has the form

$$\begin{aligned} & [\xi(i_m, j_m, i_n, j_n)]_{\text{numerical}} \\ &= \sum_{p=1}^{NGL_{mu}} \sum_{q=1}^{NGL_{mv}} \sum_{s=1}^{NGL_{nu}} \sum_{t=1}^{NGL_{nv}} A_p A_q A_s A_t u_{m,p}^{i_m} v_{m,q}^{j_m} u_{n,s}^{i_n} v_{n,t}^{j_n} \\ & \cdot g[|\mathbf{r}_m(u_{m,p}, v_{m,q}) - \mathbf{r}_n(u_{n,s}, v_{n,t})|] \end{aligned} \quad (1)$$

where  $NGL_{mu}$ ,  $NGL_{mv}$ ,  $NGL_{nu}$ , and  $NGL_{nv}$  are the adopted orders,  $u_{m,p}$ ,  $v_{m,q}$ ,  $u_{n,s}$ , and  $v_{n,t}$  are arguments (zeros of the Legendre polynomials), and  $A_p$ ,  $A_q$ ,  $A_s$ , and  $A_t$  are weights of the corresponding Gauss-Legendre integration formulas. Of course, since the integrand contains Green's function, it is not a polynomial (in parametric coordinates), and the well-known accuracy characterizations of the quadrature formula—if applied to integrals of polynomials—do not apply here [the integrand of FEM integrals is not a polynomial in  $u$ ,  $v$ , and  $w$  either].

### III. PROCEDURE FOR DETERMINING OPTIMAL HIGHER ORDER MODELING PARAMETERS THROUGH NUMERICAL EXPERIMENTS

We investigate the behavior of higher order MoM-SIE and FEM-MoM numerical solutions by running an exhaustive series of electromagnetic simulations of several canonical models of metallic and dielectric scatterers, in which we systematically vary the key higher order modeling parameters: number of elements in the model,  $M$  ( $h$ -refinement), or, equivalently, numbers of subdivisions per edge,  $H_u$ ,  $H_v$ , and  $H_w$ , of initially used elements, polynomial orders of basis (and testing) functions,  $N_u$ ,  $N_v$ , and  $N_w$  ( $p$ -refinement), orders of Gauss-Legendre integration formulas, i.e., numbers of integration points,  $NGL_u$ ,  $NGL_v$ , and  $NGL_w$  in (1) to solve MoM and FEM integrals (integration accuracy), and geometrical orders of elements, namely, orders of Lagrange-type curvature in the model,  $K_u$ ,  $K_v$ , and  $K_w$  (when curved elements are employed).

However, the combinatorial space of the adopted key parameters is enormously vast and technically ungraspable, particularly when one takes into account that all of the parameters can generally be changed anisotropically along the element (quadrilateral or hexahedron) edges. Hence, in the study, we limit this space by using only elements with isotropic polynomial orders,  $N_u = N_v = N$  for MoM quadrilaterals and  $N_u = N_v = N_w = N$  for FEM hexahedra, and similarly  $NGL_u = NGL_v = NGL$

for quadrilaterals and  $NGL_u = NGL_v = NGL_w = NGL$  for hexahedra, as well as  $K_u = K_v = K$  and  $K_u = K_v = K_w = K$ , respectively. In addition, meshes in all examples are refined isotropically in all directions: the initial, roughest, geometrical mesh is equally subdivided along all edges in the  $h$ -refinement process ( $H_u = H_v = H_w = H$ ). Finally, the same set of parameters is adopted (and then equally varied) in all elements in a model. These restrictions impose the utilization of simple symmetric structures to be analyzed as EM models for the given purpose. Hence, the structures to be modeled and simulated are chosen to be metallic and homogeneous dielectric cubical and spherical scatterers, respectively. Nonetheless, the number of simulations (and obtained results) with systematically varying (i) the number of edge divisions from  $H = 1$  to  $H = 3$ , (ii) polynomial orders of basis (and testing) functions from  $N = 1$  to  $N = 10$ , and (iii) orders of Gauss-Legendre formulas from  $NGL = 2$  to  $NGL = 20$ , as well as (iv) using the curvature orders (for spheres) of  $K = 2$  and  $K = 4$ , respectively, is still extremely large and entirely sufficient for drawing the desired conclusions.

In higher order computational models, we define the model mesh complexity by referring to the number of quadrilateral patches on the structure side,  $E = H \times H$ . For instance, a cube or a sphere modeled by only one patch per side is defined by  $E = 1 \times 1$ , which results in a total of  $6 \times 1 \times 1 = 6$  patches (and  $1 \times 1 \times 1 = 1$  FEM element in the FEM-MoM model). The refined mesh determined by  $E = 2 \times 2$  is the one with initial side patches divided into  $2 \times 2$  quadrilaterals, yielding a total of  $6 \times 2 \times 2 = 24$  patches (the corresponding number of FEM elements in such a mesh would be  $2 \times 2 \times 2 = 8$ ). Similarly, an  $E = 3 \times 3$  model has  $6 \times 3 \times 3$  patches. Additionally, cube side length and sphere radius for the considered scatterers are both set to  $a = 1$  m and the relative dielectric permittivity of dielectric scatterers is adopted to be  $\epsilon_r = 4$  in all examples and experiments. When referring to the electrical size of the model, we consider  $a/\lambda_0$  for metallic and  $a/\lambda$  for dielectric scatterers, where  $\lambda_0$  and  $\lambda$  are the wavelengths in free space and in the dielectric of the object, respectively. Finally, we adopt only single machine precision for all computations, having in mind, however, that this is one of the key limiting factors for both accuracy and convergence with  $h$ -,  $p$ -, and integral accuracy refinements, and that quantitative recipes for adoptions of optimal higher order modeling parameters would be different in double (or higher) precision.

Cubical scatterers (metallic and dielectric) are excellent benchmarking choices because their geometry can be modeled exactly, thus eliminating the geometrical error from the numerical solution. They are attractive for evaluation of numerical methods also because of their sharp edges and corners, in the vicinity of which the fields and currents exhibit singular, and challenging to model and capture, behavior. Although analytical solutions do not exist for these models, experimental results and highly accurate numerical solutions, obtained by one of the industry's leading commercial software tools for full wave EM analysis—WIPL-D, are used for validations and comparisons. In that, to avoid trade-offs between accuracy and run-time, standard for commercial codes, all WIPL-D reference models are constructed using the fully manual expert mode, in

which meshes are built manually, point-by-point (all elements in models are manually defined, with no automatic meshing or subdivision allowed), all element current expansions and integration accuracies are manually chosen, and solutions are fully *hp*-refined and carefully checked for convergence in a considered frequency range. Spherical scatterers, on the other hand, are excellent evaluation and benchmarking models because the analytical solutions for them exist in the form of Mie's series, allowing exact validation of numerical solutions and rigorous judging of the numerical accuracy. Additionally, they are objects with pronounced curvature, which is always a challenge for modeling from the geometrical point of view (in fact, spheres are customarily taken as examples of difficulties with modeling of curvature by many researchers). Spherical scatterers are therefore convenient for analysis of higher order solutions involving curved large-domain Lagrange-type quadrilaterals and hexahedra.

The direct solution to EM (scattering) problems analyzed by the MoM-SIE technique is the (equivalent) surface current distribution on the scatterer surface(s). The quality of the solution can thus be most naturally (from the mathematical point of view) judged by examining an error associated with the current distribution (e.g., in an average or an RMS sense). However, in this paper, we take a more practical approach and adopt the radar cross-section (RCS), which is most frequently the quantity of interest that is measured and simulated in real EM scattering applications, to be the quantity of choice for our assessment of the solution accuracy. We also construct a simple metric, the absolute RCS error in dB, for error evaluation. We evaluate the absolute RCS error in FEM-MoM computations as well.

To cope with the still abundantly large number of possible parameter variations and experimentation scenarios, we adopt the following systematic analysis procedure and strategy. In all examples, we start with the simplest model ( $E = 1 \times 1$ ) and analyze (a) the absolute monostatic RCS error, computed as  $|RCS_{\text{numerical}} - RCS_{\text{reference}}|$  in dB, for a fixed high  $NGL$  ( $NGL = 20$ ) vs. the model electrical size and (b) the average absolute RCS error, averaged over multiple electrical sizes of elements in a reasonable frequency range, where the elements are electrically small enough to yield accurate solutions, vs.  $NGL$ . Both analyses are carried out for a series of polynomial orders  $N$ , and respective families of curves are generated. In analysis of the error vs. the model size [analysis (a)], we seek, for every  $N$ , the  $a/\lambda$  (or  $a/\lambda_0$ ) limit for which the model yields a solution with an error not significantly higher than 0.1 dB (in graphs, we truncate the error curves when the error becomes much higher than 1 dB—for the clarity of the graph) and note how this limit increases with increasing  $N$  (*p*-refinement). In analysis of the average error vs.  $NGL$  [analysis (b)], we seek the optimal  $N$ , for which the average error is small enough (below 0.1 dB) and does not improve much with further *p*-refinement, and the corresponding  $NGL$ . We consider the accuracy of RCS simulation results with an error lower than 0.1 dB to be excellent in terms of practical relevance, since the minimum uncertainty (error) in RCS measurements and calibrations is almost never at or below the 0.2 dB level [25]–[27], and the errors lower than 0.1

dB are practically undetectable. In other words, based on the obtained results, we draw conclusions about the convergence of the results with increasing  $N$  (*p*-refinement), maximum electrical size of the elements,  $e$  (in terms of  $\lambda$  or  $\lambda_0$ ), that can be analyzed using sufficiently high  $N$  (beyond which *h*-refinement should be performed), the highest  $N$  that can be reasonably used, and the optimal  $N$  and  $NGL$ . We then *h*-refine the model mesh and repeat the procedure. For spheres, we go through the same steps using curved Lagrange-type elements with fixed  $K = 2$  and  $K = 4$ , respectively. Finally, we perform higher order RCS analysis of the NASA almond [28], which is an EMCC (Electromagnetic Code Consortium) benchmark target and one of the most popular benchmarking examples for both research and commercial CEM codes, as well as higher order MoM-SIE input-impedance computation for a wire-plate antenna.

#### IV. NUMERICAL RESULTS AND DISCUSSION: OPTIMAL MODELING PARAMETERS AND PARAMETER LIMITS

##### A. Optimal Higher Order Modeling Parameters for MoM-SIE Scattering Analysis of a Metallic Cube

We first present the higher order MoM-SIE scattering analysis of a metallic (PEC) cube (with  $a = 1$  m), starting with the simplest model ( $E = 1 \times 1$ ) of the scatterer. Based on the results in Fig. 3(a), we conclude that the model is accurately simulated up to a limit of  $a/\lambda_0 = 2$  (element edge size amounts to  $e = 2\lambda_0$ ) using  $N = 6$  or (depending on the desired accuracy level) up to  $a/\lambda_0 = 3$  with  $N = 7$ , and that even a model as large as  $a/\lambda_0 = 3.5$  in electrical size of the element edge may be considered to be usable (for some engineering applications) if  $N = 8$  is employed. From Fig. 3(b), where, for the average error, we take into account the conservative maximum element size (before *h*-refinement) of  $e = 2\lambda_0$ , we realize (looking at the “knee” points of the curves) that  $NGL = N + 2$  is optimal for all orders  $N$  ( $N = 5, 6, 7$ , and 8) providing very accurate results (error smaller than 0.1 dB). Orders  $N > 8$  are not recommended as they do not yield better results—they neither significantly increase the analyzable model size nor improve the average accuracy of the solution in the reasonable frequency range. Based on all of the above, we select the overall optimal choice of parameters to be  $N = 6$  and  $NGL = 8$  (for  $e = 2\lambda_0$ ), and compute and plot the normalized RCS ( $RCS/\lambda_0^2$ ) in Fig. 3(c), where we also plot the results for  $N = 8$  and  $NGL = 10$  for the less conservative maximum element size ( $e = 3\lambda_0$ ), as well as the measured RCS [29]. If elements smaller than optimal have to be used, which may be mandated by the geometrical or material complexity of the structure under consideration, the optimal polynomial orders are reduced by one for every reduction of the element size by  $0.5\lambda_0$ ; for instance, based (preliminary) on Fig. 3(a),  $N = 5$  is optimal for  $\lambda_0 < e \leq 1.5\lambda_0$ , while  $N = 4$  is the best choice if  $0.5\lambda_0 < e \leq \lambda_0$  (this will be explored more in studies with *hp*-refinements).

We then *h*-refine the cube model mesh to  $E = 2 \times 2$  and repeat the procedure. From the results in Fig. 4(a), we see that the model is accurately analyzed up to  $a/\lambda_0 = 4$  ( $e = 2\lambda_0$ ) using  $N = 6$ , and even to  $a/\lambda_0 = 6$  ( $e = 3\lambda_0$ ) with  $N = 8$ . Based on Fig. 4(b), we conclude that—for  $N = 5, 6, 7$ , and

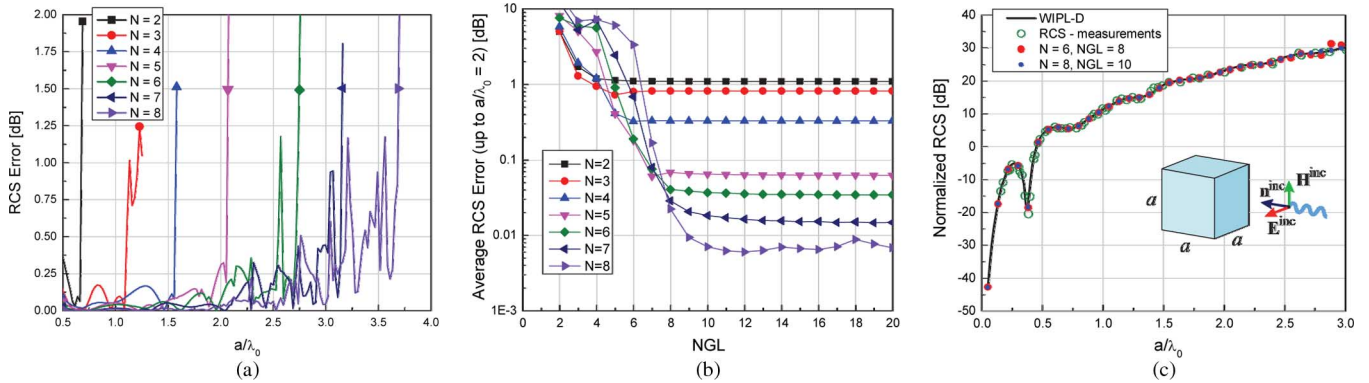


Fig. 3. Higher order MoM-SIE scattering analysis of a metallic cube with  $E = 1 \times 1$  ( $K = 1$ ): (a) absolute RCS error for  $NGL = 20$  and a series of orders  $N$  ( $p$ -refinement) vs. the model electrical size, (b) absolute RCS error averaged over multiple values of  $a/\lambda_0$  in a frequency range corresponding to reasonable model sizes,  $a/\lambda_0 \leq 2$  (conservative maximum model size), with a series of  $N$  values vs.  $NGL$ , and (c) the optimal solution ( $N = 6$  and  $NGL = 8$  for  $e = 2\lambda_0$ ), along with the results for  $N = 8$  and  $NGL = 10$  (for  $e = 3\lambda_0$ ) and measured data [29].

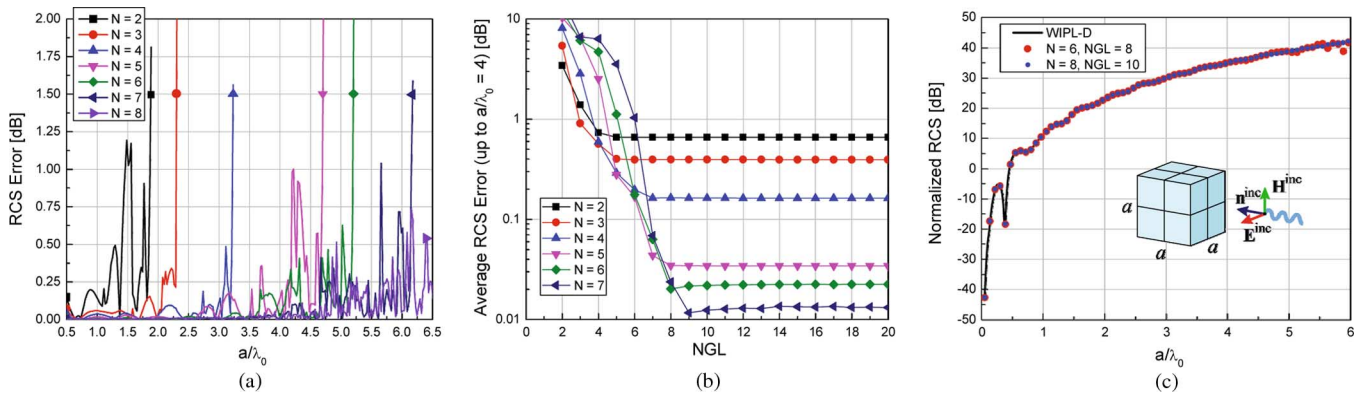


Fig. 4. MoM-SIE analysis of a metallic cube with  $E = 2 \times 2$ : (a) RCS error for  $NGL = 20$  and  $p$ -refinement, (b) average RCS error for reasonable model sizes,  $a/\lambda_0 \leq 4$ , with  $p$ -refinement vs.  $NGL$ , and (c) the optimal solution for both  $N = 6$  ( $e = 2\lambda_0$ ) and  $N = 8$  ( $e = 3\lambda_0$ ).

8— $NGL = N + 2$  is optimal (“knees” of curves), as well as that the optimal polynomial order is again  $N = 6$  (with  $NGL = 8$ ), while orders  $N = 9$  and higher are not recommended. The normalized RCS for the more conservative ( $N = 6$ ,  $e = 2\lambda_0$ ) and less conservative ( $N = 8$ ,  $e = 3\lambda_0$ ) optimal solutions is shown in Fig. 4(c).

Finally, for  $E = 3 \times 3$ , the results in Fig. 5(a) tell us that the model is accurate up to  $a/\lambda_0 = 6$  ( $e = 2\lambda_0$ ) for  $N = 6$ , and even higher (for  $N = 7$ ). From Fig. 5(b),  $NGL = N + 2$  is optimal, for  $N = 5, 6$ , and  $7$ , and the optimal  $N$ , for  $e = 2\lambda_0$ , comes out to be  $N = 6$  (with  $NGL = 8$ ). Fig. 5(c) shows the optimal solution for both  $e = 2\lambda_0$  and  $e = 3\lambda_0$ . Note that the solution with  $N = 6$  and  $NGL = 8$  requires 3888 unknowns and takes 16.27 s of computation time at a single frequency using a PC with Intel Core 2 Quad CPU Q6600 at 2.4 GHz, 8.00 GB of RAM, and 64-bit Microsoft Windows 7. In addition, Fig. 6(a) tells us that if elements up to  $e = 0.5\lambda_0$  in size are used, orders  $N = 2$  or  $3$  provide accurate results,  $N = 3$  or  $4$  suffices, based on Fig. 6(b), for  $e \leq \lambda_0$ , and  $N = 4$  or  $5$  should be used if the maximum element size in the model is  $e = 1.5\lambda_0$ , Fig. 6(c), where, in all cases,  $NGL = N + 2$  (“knee” points of the curves) is the optimal choice.

General conclusions for the higher order MoM-SIE scattering analysis of a metallic cube are that the optimal (or nearly optimal) choice of polynomial orders of basis and testing functions

and orders of Gauss-Legendre integration formulas is given by  $N = 6$  and  $NGL = 8$ , respectively. The mesh should be  $h$ -refined if the element edge size becomes greater than  $e = 2\lambda_0$  (conservative option). If elements smaller than optimal are to be used, the optimal polynomial orders are  $N = 2$  for  $e \leq 0.25\lambda_0$ ,  $N = 3$  for  $0.25\lambda_0 < e \leq 0.5\lambda_0$ ,  $N = 4$  for  $0.5\lambda_0 < e \leq \lambda_0$ ,  $N = 5$  for  $\lambda_0 < e \leq 1.5\lambda_0$ , and  $N = 6$  for  $1.5\lambda_0 < e \leq 2\lambda_0$ . Hence, the minimum average total number of unknowns (the number of current expansion coefficients for the whole model) per wavelength for accurate RCS analysis amounts approximately to 11.3 if  $N = 2$  is used, to 8.5 if  $N = 3$ , to 5.7 for  $N = 4$ , to 4.7 for  $N = 5$ , and to 4.2 if  $N = 6$  is implemented in the model. Orders  $N > 8$  are not recommended to be used ( $h$ -refinement should be performed instead). It is generally optimal to use  $NGL = N + 2$  for any  $N$ . It is generally not recommended to increase  $NGL$  any further, except in order to verify the solution stability.

### B. Optimal Higher Order Modeling Parameters for MoM-SIE Scattering Analysis of a Dielectric Cube

Next, we carry out the numerical investigation of higher order modeling parameters in the MoM-SIE analysis of a dielectric cube scatterer (with  $a = 1$  m and  $\epsilon_r = 4$ ). For the simplest model ( $E = 1 \times 1$ ), results in Fig. 7(a) indicate that the computation is accurate up to  $a/\lambda = 2$  (element edge size is  $e = 2\lambda$ )

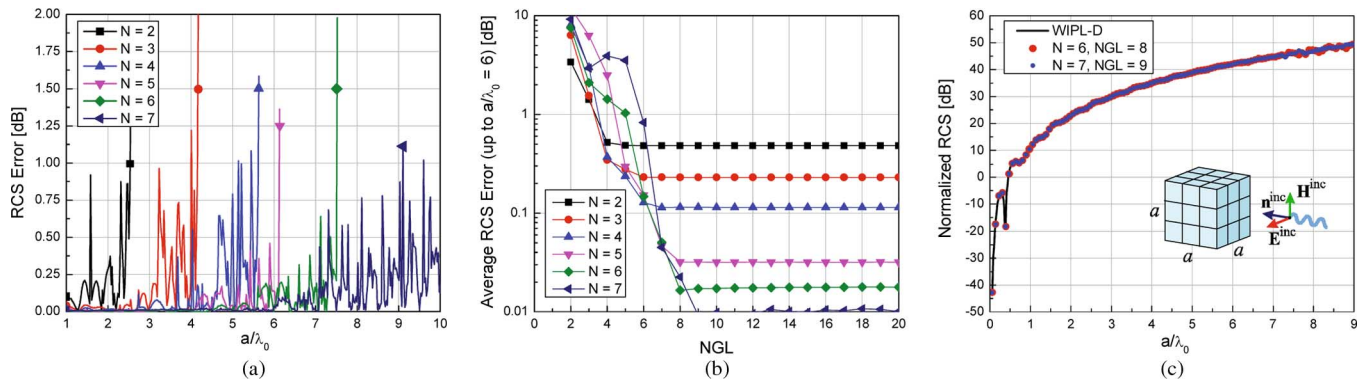


Fig. 5. MoM-SIE simulations of a metallic cube with  $E = 3 \times 3$ : (a) RCS error vs.  $a/\lambda_0$  ( $NGL = 20$ ), (b) RCS error averaged over reasonable model sizes up to  $a/\lambda_0 = 6$  or  $e = 2\lambda_0$  (conservative choice), and (c) the optimal solution (for both  $e = 2\lambda_0$  and  $e = 3\lambda_0$ ).

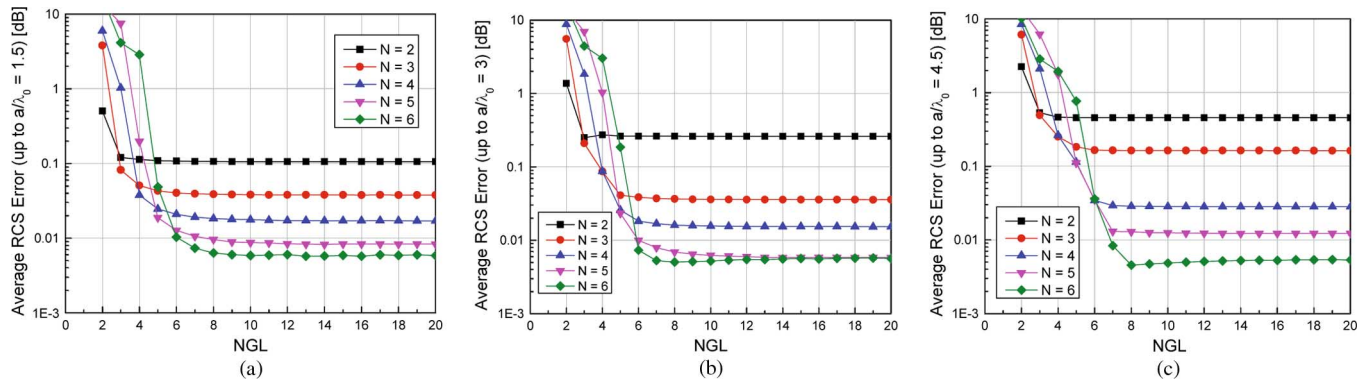


Fig. 6. Average RCS error in the MoM-SIE analysis of a metallic cube with  $E = 3 \times 3$  for (a)  $e \leq 0.5\lambda_0$ , (b)  $e \leq \lambda_0$ , and (c)  $e \leq 1.5\lambda_0$ .

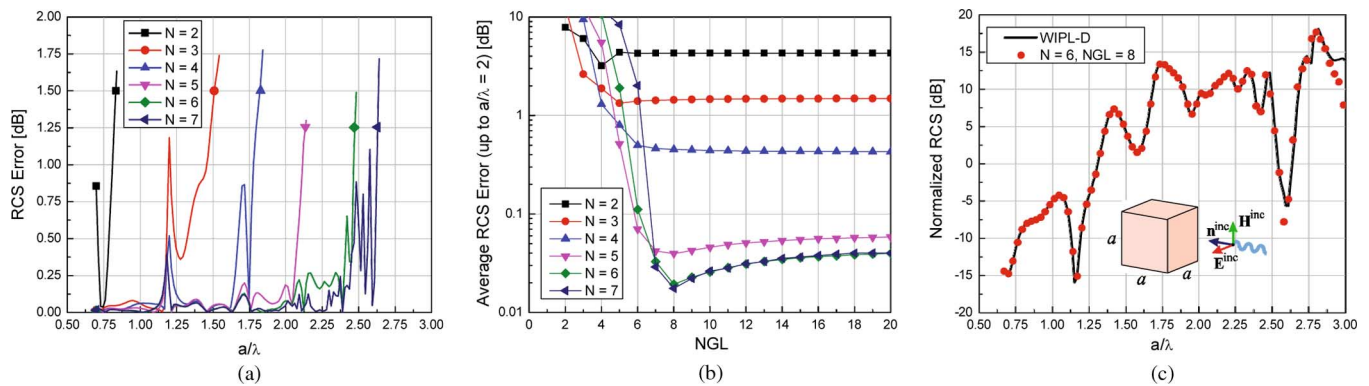


Fig. 7. Higher order MoM-SIE computation of a dielectric cube scatterer with  $E = 1 \times 1$ : (a) absolute RCS error for  $NGL = 20$  and  $p$ -refinement vs. the model electrical size, (b) absolute RCS error averaged over multiple reasonable model sizes,  $a/\lambda \leq 2$ , with  $p$ -refinement vs.  $NGL$ , and (c) the optimal solution (the results are shown also beyond the reasonable range, i.e., up to  $a/\lambda = 3$ ).

using  $N = 5$  or  $6$ , while adoption of a larger  $N$  can extend the analyzable size even further. According to Fig. 7(b), we realize that the polynomial orders  $N = 5$  or  $6$  are optimal, for  $NGL = N + 2$  (see the “knee” points of the curves), while orders  $N = 7$  and higher are not recommended. The normalized RCS of the cube using the optimal set of parameters  $N = 6$  and  $NGL = 8$  is shown in Fig. 7(c).

For the mesh with  $E = 2 \times 2$ , the results in Fig. 8(a) are accurate up to  $a/\lambda = 4$  ( $e = 2\lambda$ , again) for  $N = 6$ . Using  $N = 7$  increases this range up to  $a/\lambda = 4.5$ . From Fig. 8(b), we conclude that  $NGL = N + 2$  is consistently optimal, as well as that the optimal polynomial order is again  $N = 6$ , while

orders  $N = 7$  and higher are not recommended. The optimal solution is presented in Fig. 8(c). We also see, in Fig. 8(a), that  $N = 2$  or  $3$  is optimal for  $e \leq 0.5\lambda$  ( $a/\lambda \leq 1$ ),  $N = 4$  is the best choice for  $0.5\lambda < e \leq \lambda$ , and  $N = 5$  should be adopted for  $\lambda < e \leq 1.5\lambda$ .

Results in Fig. 9 for the model of the dielectric cube scatterer with  $E = 3 \times 3$  yield identical conclusions as those in Fig. 8. Here, the number of unknowns and computation time for the solution with  $N = 6$  and  $NGL = 8$  are 7776 and 144 s, respectively.

Overall, the conclusions are practically the same as in the analysis of metallic scatterers, that  $N = 6$  and  $NGL = 8$

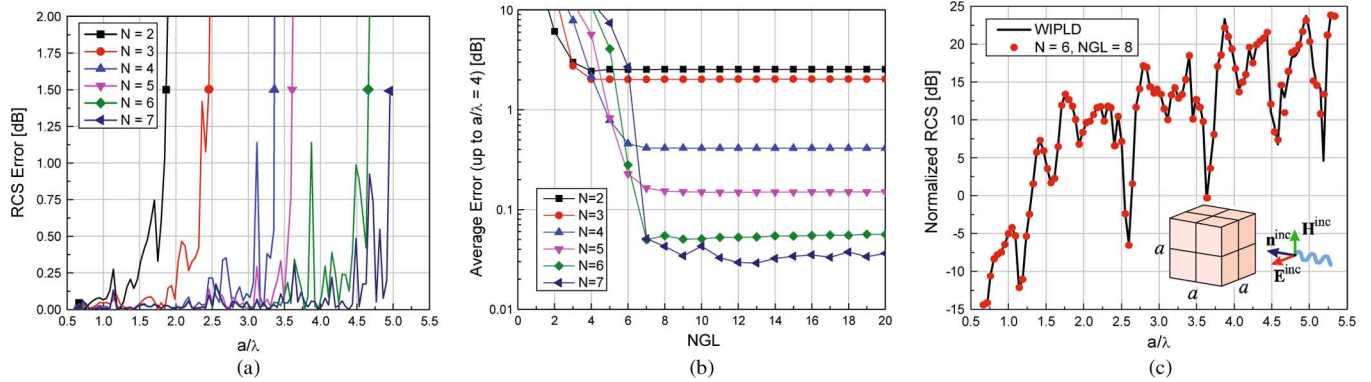


Fig. 8. MoM-SIE simulations of a dielectric cube with  $E = 2 \times 2$ : (a) RCS error vs. the model electrical size ( $NGL = 20$ ), (b) average RCS error for reasonable model sizes,  $a/\lambda \leq 4$ , vs.  $NGL$ , and (c) the optimal solution (shown within the reasonable range and above it, up to  $a/\lambda = 5.5$ ).

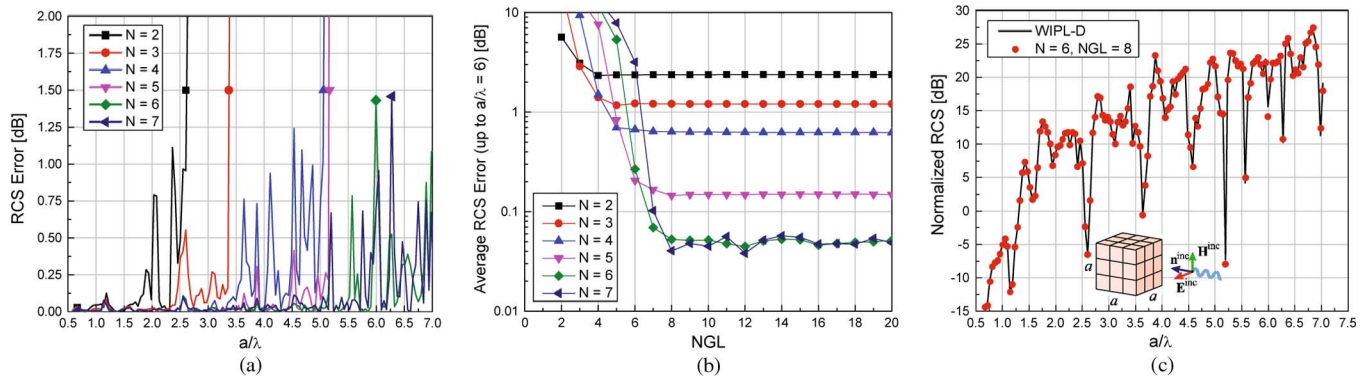


Fig. 9. MoM-SIE analysis of a dielectric cube with  $E = 3 \times 3$ : (a) RCS error ( $NGL = 20$ ), (b) average RCS error for reasonable model sizes up to  $a/\lambda = 6$ , and (c) the optimal solution (shown across and beyond the reasonable range).

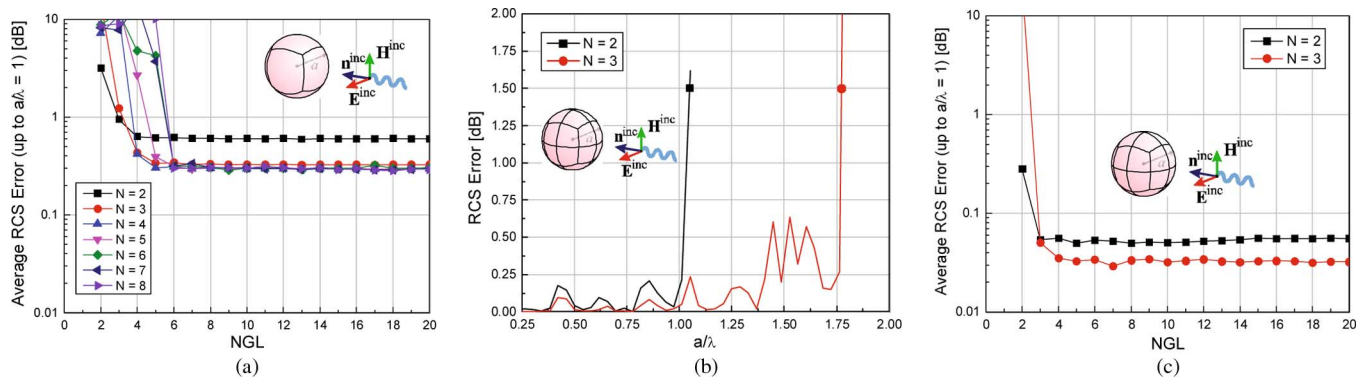


Fig. 10. Higher order MoM-SIE analysis of a dielectric spherical scatterer with  $K = 2$ : (a) average RCS error for  $E = 1 \times 1$  and  $p$ -refinement (unsuccessful) vs.  $NGL$ , (b) RCS error for  $E = 2 \times 2$ ,  $NGL = 20$ , and two lower values of  $N$  vs. the model electrical size, and (c) RCS error for  $E = 2 \times 2$  averaged for multiple reasonable model sizes,  $d/\lambda \leq 2$ , vs.  $NGL$ .

constitute the optimal (or very close to optimal) choice for MoM-SIE expansion polynomial orders and numbers of Gauss-Legendre integration points, respectively, that the mesh should be refined for elements larger than  $e = 2\lambda$  in edge length, which corresponds to the conservative maximum element edge length selection for metallic scatterers of  $e = 2\lambda_0$ , that the optimal orders  $N$  are reduced by one for every reduction of the element size by  $0.5\lambda$  if elements smaller than optimal have to be used, and that setting  $NGL = N + 2$  is generally optimal for any  $N$ . In addition, note that for the generally optimal choice of  $N = 6$ , the computation time for the analysis of an  $E = 1 \times 1$  dielectric cube in 100 frequency

points is 31% longer if  $NGL = N + 4$  is used instead of the generally optimal  $NGL = N + 2$ , and if a “brute-force” adoption of  $NGL = 20$  is employed, the simulation time is 742% longer.

### C. Optimal Higher Order Modeling Parameters for MoM-SIE Scattering Analysis of a Dielectric Sphere

The next example is a dielectric spherical scatterer (with  $a = 1$  m and  $\epsilon_r = 4$ ) analyzed using the higher order MoM-SIE technique, and the first geometrical model is characterized by  $E = 1 \times 1$  and  $K = 2$ . From the results in Fig. 10(a), we realize

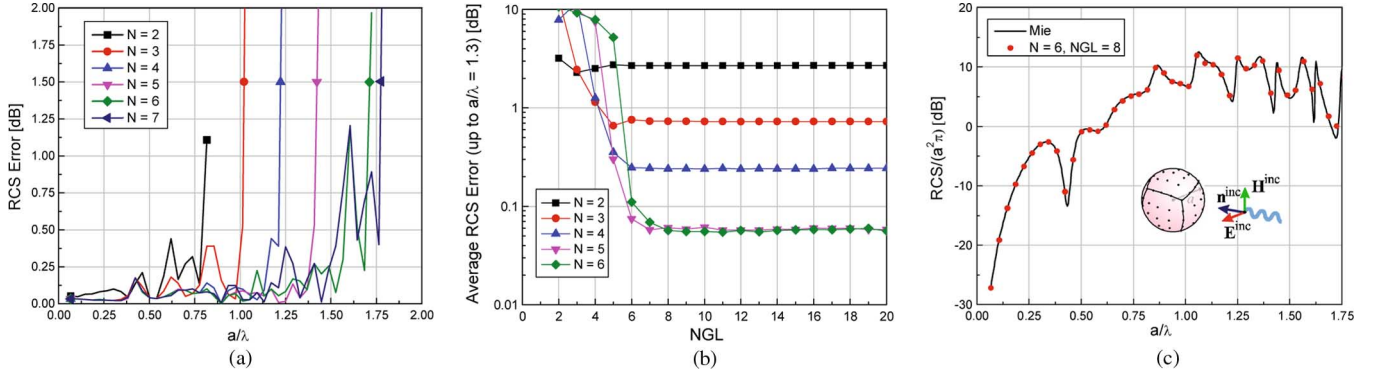


Fig. 11. MoM-SIE scattering computation of a dielectric sphere with  $E = 1 \times 1$  and  $K = 4$ : (a) RCS error vs. the model electrical size ( $NGL = 20$ ), (b) average RCS error for reasonable model sizes up to  $d/\lambda = 2.6$  vs.  $NGL$ , and (c) the optimal solution (shown within and above the reasonable range).

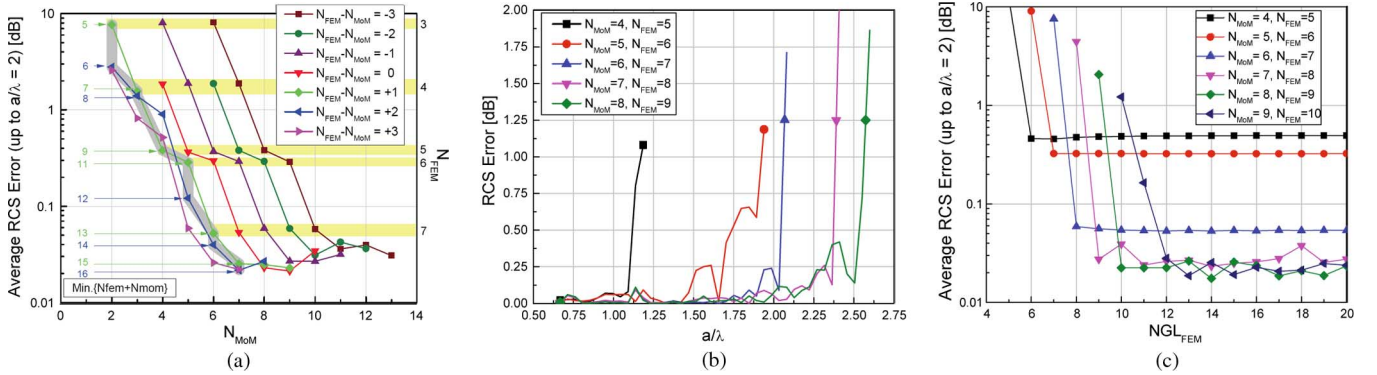


Fig. 12. Higher order FEM-MoM scattering analysis of a dielectric cube with  $E = 1 \times 1$ : (a) RCS error averaged for multiple reasonable model sizes, up to  $a/\lambda = 2$ , for different polynomial orders  $N_{FEM}$  and  $N_{MoM}$ . (b) absolute RCS error for a series of values for  $N_{FEM}$  ( $N_{FEM} - N_{MoM} = 1$ ) vs. the electrical size of the scatterer ( $NGL_{FEM} = 20$  and  $NGL_{MoM} = 19$ ), and (c) average RCS error for reasonable model sizes,  $a/\lambda \leq 2$ , with  $p$ -refinement vs.  $NGL$  ( $NGL_{FEM} - NGL_{MoM} = 1$ ).

that the solution accuracy is limited by the accuracy of the geometrical model, and that it cannot be improved by  $p$ -refinement. For an  $h$ -refined model with  $E = 2 \times 2$  and  $K = 2$ , we observe, in Fig. 10(b), that the model enables accurate simulations up to  $a/\lambda = 1$  or  $d/\lambda = 2$  ( $d$  is the diameter of the sphere), with the elements being about  $e = 0.8\lambda$  across, for  $N = 2$ , and up to  $a/\lambda = 1.75$  or  $d/\lambda = 3.5$  ( $e = 1.4\lambda$ ) for  $N = 3$ , while, based on Fig. 10(c),  $NGL = N + 1$  is an optimal choice. High-order basis functions ( $N \geq 4$ ) cannot be efficiently used due to the geometrical inaccuracy of the model.

We then increase the element geometrical orders in the  $E = 1 \times 1$  model of the sphere to  $K = 4$  and repeat the procedure. Results in Fig. 11(a) indicate that the model can now be accurately simulated up to at least  $a/\lambda = 1.3$  or  $d/\lambda = 2.6$  ( $e = 2\lambda$ ) with  $N = 6$ . According to Fig. 11(b), the average RCS error is very small (0.068 dB) for  $N = 4$  and  $NGL = 6$ , and does not improve much with further  $p$ -refinement, due to small geometrical inaccuracy (e.g., setting  $N = 6$  and  $NGL = 8$  yields a 0.057 dB error), while generally optimal orders of Gauss-Legendre integration formulas are (observing the “knees” of the respective curves)  $NGL = N + 2$  (for any  $N$ ). It turns out that we can now take advantage of high-order basis functions due to significantly higher geometrical accuracy of the model than with  $K = 2$ . However, orders  $N \geq 8$  are not recommended, since they do not yield better average errors. The optimal solution, for  $N = 6$ , is given in Fig. 11(c). Note that all conclusions are essentially the same as for the dielectric cube. Note also that

the same conclusions are obtained for a metallic (PEC) spherical scatterer as well.

#### D. Optimal Higher Order Modeling Parameters for FEM-MoM Scattering Analysis of a Dielectric Cube

We next conduct a numerical study of higher order modeling parameters in the hybrid FEM-MoM scattering analysis of a dielectric cube ( $a = 1$  m and  $\epsilon_r = 4$ ), adopting the simplest model possible, with  $E = 1 \times 1$  (one FEM and six MoM elements). We sweep polynomial orders for FEM field expansions from  $N_{FEM} = 3$  to 11 and for MoM current expansions from  $N_{MoM} = 2$  to 13, keeping a conservative choice of orders of Gauss-Legendre integration formulas given by  $NGL_{MoM} = N_{MoM} + 4$  (higher than optimal according to the MoM-SIE studies) and adopting the same choice for the FEM part,  $NGL_{FEM} = N_{FEM} + 4$ . Fig. 12(a) shows that the minimal order sums  $N_{FEM} + N_{MoM}$  (thick gray curve) for any given error are achieved when parameter  $N_{FEM} - N_{MoM}$  equals 1 or 2. However, we realize that  $N_{FEM}$  is the accuracy limiting factor (light yellow areas), and hence the choice that gives the minimal order sum is  $N_{FEM} - N_{MoM} = 1$  (green curve). Note that the light yellow ribbons (constant  $N_{FEM}$ ) are depicted for the first five curves only (excluding the blue and magenta curves). These ribbons would be shifted higher (larger error) for the  $N_{FEM} - N_{MoM} = +2$  curve and even higher for the  $N_{FEM} - N_{MoM} = +3$  curve. So, the conclusion is that the optimal order separation between  $N_{FEM}$  and

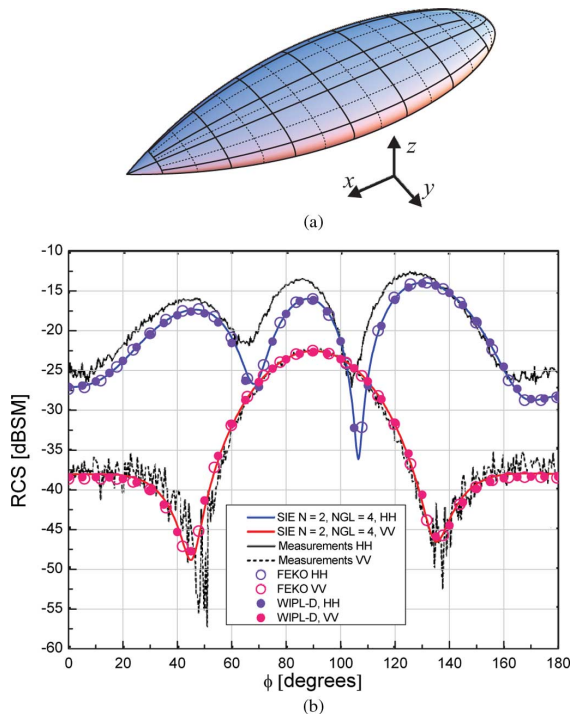


Fig. 13. Higher order MoM-SIE scattering analysis of the NASA metallic almond at  $f = 1.19$  GHz [28]: (a) geometrical model with  $M = 56$  curved ( $K = 2$ ) quadrilateral elements and (b) comparison of the simulation results for the RCS of the almond as a function of the azimuthal angle (the elevation angle is zero) for the horizontal (HH) and vertical (VV) polarizations, respectively, with the numerical results obtained by WIPL-D and FEKO [30], as well as with the results of measurements [28].

$N_{\text{MoM}}$  is unity. This can be attributed to the fact that dominant FEM-MoM inner products are normally those between FEM and MoM basis functions in the same direction, whose maximal orders are offset by one in the mixed-order arrangement for curl-conforming FEM functions with respect to that for divergence-conforming MoM functions [12].

Finally, to determine the optimal  $NGL$  and  $N$  in the FEM-MoM analysis, we simulate the same dielectric scatterer employing the optimal  $N_{\text{FEM}} - N_{\text{MoM}} = 1$  and systematically varying  $N_{\text{FEM}}$  from 5 to 10, and plot the graphs in Figs. 12(b) and (c). To reduce the number of combinations and computations, we also adopt  $NGL_{\text{FEM}} - NGL_{\text{MoM}} = 1$ . Based on Fig. 12(b), we conclude that the cube can be very accurately analyzed up to  $a/\lambda = 2$  ( $e = 2\lambda$ ) using  $N_{\text{FEM}} = 7$  and  $N_{\text{MoM}} = 6$ . From Fig. 12(c), on the other side, we obtain that the generally optimal  $NGL_{\text{FEM}}$  (“knees” of the curves) is  $NGL_{\text{FEM}} = N_{\text{FEM}} + 1$  for any  $N_{\text{FEM}}$  (but higher  $NGL$ s can be used as well), and that the overall optimal orders come out to be  $N_{\text{FEM}} = 7$ ,  $N_{\text{MoM}} = 6$ ,  $NGL_{\text{FEM}} = 8$ , and  $NGL_{\text{MoM}} = 7$ . This conclusion is consistent with conclusions drawn for the same scatterer analyzed by the MoM-SIE technique, where  $N_{\text{MoM-SIE}} = 6$  and  $e = 2\lambda$  is the optimal choice as well.

#### E. Higher Order MoM-SIE RCS Analysis of the NASA Almond

As the last scattering example, we analyze a scatterer where, due to the geometrical complexity and constraints of the structure, electrically relatively small elements have to

be used—namely, we perform higher order MoM-SIE RCS analysis of the NASA almond, a benchmark target established by the Electromagnetic Code Consortium (EMCC), at a frequency of  $f = 1.19$  GHz [28]. Fig. 13(a) shows a model of the almond built (based on geometrical equations from [28]) using  $M = 56$  quadrilateral curved elements with  $K = 2$ ,  $N = 2$ , and  $NGL = 4$  (all elements are in the  $e \leq 0.25\lambda_0$  range), resulting in a total of only 448 unknowns (with no use of symmetry). The higher order simulation results for the RCS of the almond are compared in Fig. 13(b) with the results obtained by WIPL-D and FEKO [30], respectively, as well as with measurements [28]. We observe an excellent mutual agreement of the three sets of numerical results and their good agreement with the measurements—for the parameters in the higher order model selected exactly according to the established recipes for adoption of higher order modeling parameters for elements smaller than optimal.

#### F. Higher Order MoM-SIE Impedance Computation for a Wire-Plate Antenna

As the final example, we perform higher order MoM-SIE analysis of a thin wire monopole antenna mounted on a square PEC plate, as shown in Fig. 14(a), in order to verify that the general guidelines and recipes for adoptions of optimal higher order simulation parameters obtained in RCS calculations also apply when a more sensitive error measure, that of the antenna input impedance, is observed. The plate edge length is  $a = 1$  m, the monopole length is  $L_m = 93.75$  mm, and its radius is  $r = 0.5$  mm. The monopole is excited at its base by a point (delta-function) voltage generator. The analysis of the structure is performed using the simplest possible model of the plate, composed of four trapezoidal (triangle-like) quadrilateral patches, as depicted in Fig. 14(a), with isotropic ( $N_u = N_v = N_p$ ) polynomial orders of basis functions on all patches. The polynomial order of the axial line current along the wire is fixed at  $N_w = 4$  (to reduce the number of possible parameter variations in the model). The reference results used for comparisons and error evaluations are obtained simulating an  $h$ -refined WIPL-D model shown in Fig. 14(b), with fully converged solutions for the entire frequency range considered.

Carefully examining error plots in Figs. 14(c) and (d), one can draw essentially the same overall conclusions about higher order parameters of the antenna-impedance analysis as in scattering examples. For instance, based on the results in Fig. 14(c), we conclude that the model in Fig. 14(a) is accurately simulated, with impedance relative errors lower than about 2.5% (which is consistent with the RCS error of 0.1 dB in scattering computations), up to a limit of  $a/\lambda_0 = 2$  using  $N_p = 3$  and up to  $a/\lambda_0 = 4$  with  $N_p = 6$ , whereas a 1% accuracy can easily be achieved by somewhat reducing the patch sizes. Note that if  $a = 4\lambda_0$ , element edge sizes for each of the patches amount to  $e_1 = 4\lambda_0$ ,  $e_2 = e_3 = 2.828\lambda_0$ , and  $e_4 = 0.004\lambda_0$ , the height of the trapezoid is  $h = 2\lambda_0$ , and the patch midlines in  $u$  and  $v$  directions are both about  $2\lambda_0$  long. In addition, from Fig. 14(d), we see that a choice of  $N_p = 6$  and  $NGL_p = 8$ , with which the impedance relative error averaged over the entire frequency range in Fig. 14(c), so up to  $a/\lambda_0 = 4$ , amounts to 1%, is again

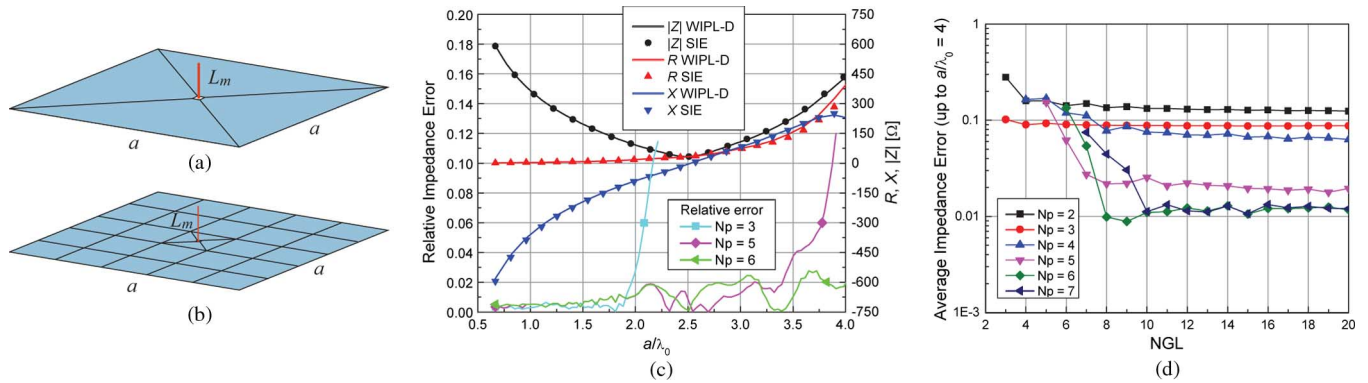


Fig. 14. Higher order MoM-SIE impedance ( $Z$ ) computation for a wire monopole antenna attached to a square plate: (a) model with four trapezoidal (triangle-like) quadrilateral patches, (b) reference WIPL-D model, (c) relative impedance error,  $\| |Z| - |Z_{reference}| \| / |Z_{reference}|$ , for  $NGL_p = NGL_w = 20$  and a series of orders  $N_p$  ( $p$ -refinement), along with the optimal ( $N_p = 6$  and  $NGL_p = 8$ ) solution for  $R$ ,  $X$ , and  $|Z|$  ( $Z = R + jX$ ), vs. the model electrical size, and (d) relative impedance error averaged over multiple values of  $a/\lambda_0$  in the entire frequency range in (c),  $a/\lambda_0 \leq 4$ , with  $p$ -refinement vs.  $NGL_p = NGL_w$ .

optimal (as in RCS calculations); the antenna impedance results plotted in Fig. 14(c) are obtained with this choice of parameters.

## V. CONCLUSIONS

This paper has investigated and evaluated the behavior of higher order hierarchical MoM-SIE and FEM-MoM numerical solutions to electromagnetic scattering problems by running an exhaustive series of simulations and systematically varying and studying the key higher order modeling parameters and their influence on the solutions. Based on numerical experiments and comprehensive case studies on symmetric canonical models that allow using elements with isotropic higher order parameters and uniform meshes (to limit the combinatorial space of the parameters in investigations), the paper has established and validated general guidelines and instructions, and as precise as possible quantitative recipes, for adoptions of optimal higher order and large-domain parameters for electromagnetic modeling, within the class of CEM approaches and techniques considered. The modeling parameters considered (note that all these parameters can, theoretically, be arbitrary) are: electrical dimensions of elements (subdivisions) in the model,  $e/\lambda$  ( $h$ -refinement), polynomial orders of basis and testing functions ( $p$ -refinement),  $N$ , orders of Gauss-Legendre integration formulas (numbers of integration points—integration accuracy),  $NGL$ , and geometrical orders of elements (orders of Lagrange-type curvature) in the model,  $K$ . In addition, higher order MoM-SIE RCS analysis of an EMCC benchmark target (NASA almond) and impedance computation for a wire-plate antenna have been performed.

Overall, the main conclusions of the study, which is the first such study of higher order parameters in CEM, can be summarized as follows. The MoM-SIE or FEM-MoM model should be  $h$ -refined if the dimensions of (flat or curved) elements become greater than  $e = 2\lambda$ , with  $\lambda$  standing for the wavelength in free space ( $\lambda_0$ ) in the case of metallic structures and for the wavelength in the dielectric for dielectric ones. The optimal (or nearly optimal) choice of orders  $N$  and  $NGL$  is given by  $N = 6$  and  $NGL = 8$ , respectively, for both metallic and dielectric structures, with or without pronounced curvature. If elements smaller than optimal have to be used, due to the geometrical or material complexity of the structure, the optimal polynomial orders should be adopted as follows:  $N = 1$  for el-

ement sizes  $e \leq 0.1\lambda$ ,  $N = 2$  for  $0.1\lambda < e \leq 0.25\lambda$ ,  $N = 3$  for  $0.25\lambda < e \leq 0.5\lambda$ ,  $N = 4$  for  $0.5\lambda < e \leq \lambda$ ,  $N = 5$  for  $\lambda < e \leq 1.5\lambda$ , and  $N = 6$  for  $1.5\lambda < e \leq 2\lambda$ . The minimum average total number of unknowns per wavelength for accurate RCS analysis amounts to about 14.1, 11.3, 8.5, 5.7, 4.7, and 4.2 if  $N = 1, 2, 3, 4, 5$ , and 6, respectively, is used in a higher order model of a PEC structure, while these numbers are doubled for dielectric scatterers. In hybrid FEM-MoM models,  $N_{FEM} - N_{MoM} = 1$  is optimal. Polynomial orders higher than  $N = 8$  are not recommended to be used. It is generally optimal to use  $NGL = N + 2$  for any  $N$ . It is generally not recommended to increase  $NGL$  any further. For curved structures,  $K = 2-4$  is always a better choice than  $K = 1$ ; for surfaces with pronounced curvature,  $K = 4$  should be adopted in order to enable efficient use of high orders  $N$  on electrically large elements, while geometrical orders higher than that are not recommended.

Established guidelines and recipes for adoptions of optimal higher order parameters in MoM and FEM simulations are quite general and applicable to a variety of electromagnetic structures and situations, but, when using them, one should have in mind the following limitations and restrictions. All conclusions are for computations in single machine precision. One of the tasks for future work along the lines of this research is to perform a study of higher order parameters for simulations in double precision, and to compare the findings for single and double precision computations. The recipes do not take into account possible high nonuniformities of fields, high geometrical and material inhomogeneities of parts of analyzed structures, and proximity effects, where additional  $h$ - and/or  $p$ -refinements may be needed to obtain accurate results (e.g., edging and imaging [31], and related procedures). The study is based primarily on far-field (RCS) evaluations of electromagnetic scatterers, with only one example of antenna input impedance calculations, which is at least indicative of the general guidelines for simulation parameters obtained in RCS simulations being applicable to current-distribution, antenna-impedance, and near-field computations as well. However, a detailed parametric study to confirm or amend these claims for near-field quantities, including the current distribution, antenna impedance, and internal field in materials, is in order for future work.

The developed set of rules should be of significant interest and value for MoM and FEM practitioners and application engineers using similar (or even not so similar) CEM software, and may result in considerable reductions of the overall simulation (modeling plus computation) time. For instance, computations involving unreasonably high or low polynomial orders of basis and testing functions and/or orders of Gauss-Legendre integration formulas, and unreasonable, too large or too small, electrical dimensions of elements in the model, as well as various unreasonable combinations of different choices, could result in meaningless models and simulations (that often cannot be refined) and/or in an unnecessarily extensive utilization of computational resources (e.g., orders of magnitude longer computation times). It should also be valuable to CEM research community in developing new higher order MoM and FEM computational methods and techniques, and to CEM software designers (e.g., in designing and building automatic or semi-automatic higher order meshes and models with optimally preset parameters).

The ultimate goal of this present work and the continued future work in this area is to reduce the dilemmas and uncertainties associated with the great modeling flexibility in higher order CEM techniques in terms of the size and shape of elements and spans of approximation and testing functions, and to ease and facilitate the decisions to be made on how to actually use them, by both CEM developers and practitioners. The goal is for the class of approaches and techniques considered here and for the higher order CEM modeling methodology in general to be an easily and confidently used analysis and design tool, with a minimum of expert interaction required to produce valuable results in practical applications. We believe that this and similar future studies, including those on associated efficient higher order meshing techniques and algorithms (which are not discussed in this paper), are the best, if not the only, way to close the large gap between the rising academic interest in the higher order CEM, which evidently shows great numerical potential, and its actual usefulness and use in electromagnetics research and engineering applications.

## REFERENCES

- [1] B. M. Notaroš, "Higher order frequency-domain computational electromagnetics," *IEEE Trans. Antennas Propag.*, vol. 56, no. 8, pp. 2251–2276, Aug. 2008.
- [2] J. M. Jin, K. C. Donepudi, J. Liu, G. Kang, J. M. Song, and W. C. Chew, "High-order methods in computational electromagnetics," in *Fast and Efficient Algorithms in Computational Electromagnetics*, W. C. Chew, Ed. Norwood, MA: Artech House, 2001.
- [3] B. M. Kolundzija and A. R. Djordjević, *Electromagnetic Modeling of Composite Metallic and Dielectric Structures*. Norwood, MA: Artech House, 2002.
- [4] A. F. Peterson, *Mapped Vector Basis Functions for Electromagnetic Integral Equations*. New York: Morgan & Claypool Publishers, 2006.
- [5] R. D. Graglia, D. R. Wilton, and A. F. Peterson, "Higher order interpolatory vector bases for computational electromagnetics," *IEEE Trans. Antennas Propag.*, vol. 45, no. 3, pp. 329–342, Mar. 1997.
- [6] G. Kang, J. Song, W. C. Chew, K. C. Donepudi, and J. M. Jin, "A novel grid-robust higher order vector basis function for the method of moments," *IEEE Trans. Antennas Propag.*, vol. 49, pp. 908–915, Jun. 2001.
- [7] M. Djordjevic and B. M. Notaros, "Double higher order method of moments for surface integral equation modeling of metallic and dielectric antennas and scatterers," *IEEE Trans. Antennas Propag.*, vol. 52, no. 8, pp. 2118–2129, Aug. 2004.
- [8] E. Jørgensen, J. L. Volakis, P. Meincke, and O. Breinbjerg, "Higher order hierarchical Legendre basis functions for electromagnetic modeling," *IEEE Trans. Antennas Propag.*, vol. 52, pp. 2985–2995, November 2004.
- [9] J. P. Webb, "Hierarchical vector basis functions of arbitrary order for triangular and tetrahedral finite elements," *IEEE Trans. Antennas Propag.*, vol. 47, no. 8, pp. 1244–1253, August 1999.
- [10] M. M. Ilic and B. M. Notaros, "Higher order hierarchical curved hexahedral vector finite elements for electromagnetic modeling," *IEEE Trans. Microw. Theory Tech.*, vol. 51, no. 3, pp. 1026–1033, Mar. 2003.
- [11] M. M. Ilic and B. M. Notaros, "Higher order large-domain hierarchical FEM technique for electromagnetic modeling using Legendre basis functions on generalized hexahedra," *Electromagnetics*, vol. 26, no. 7, pp. 517–529, Oct. 2006.
- [12] M. M. Ilić, M. Djordjević, A. Ž. Ilić, and B. M. Notaroč, "Higher order hybrid FEM-MoM technique for analysis of antennas and scatterers," *IEEE Trans. Antennas Propag.*, vol. 57, pp. 1452–1460, May 2009.
- [13] B. D. Popovic, "Polynomial approximation of current along thin symmetrical cylindrical dipoles," *IEE Proc.*, vol. 117, pp. 873–878, 1970.
- [14] B. M. Kolundzija and B. D. Popovic, "Entire-domain Galerkin method for analysis of generalized wire antennas and scatterers," *Proc. IEE H*, vol. 139, no. 1, pp. 17–24, Feb. 1992.
- [15] B. M. Kolundzija, "Comparison of a class of sub-domain and entire-domain basis functions automatically satisfying KCL," *IEEE Trans. Antennas Propag.*, vol. 44, no. 10, pp. 1362–1366, Oct. 1996.
- [16] B. M. Kolundzija, "Accurate solution of square scatterer as benchmark for validation of electromagnetic modeling of plate structures," *IEEE Trans. Antennas Propag.*, vol. 46, pp. 1009–1014, Jul. 1998.
- [17] B. M. Notaros and B. D. Popovic, "Optimized entire-domain moment-method analysis of 3D dielectric scatterers," *Int. J. Numer. Modelling: Electronic Networks, Devices Fields*, vol. 10, pp. 177–192, 1997.
- [18] V. V. Petrovic and B. D. Popovic, "Optimal FEM solutions of one dimensional EM problems," *Int. J. Numer. Modelling: Electronic Networks, Devices Fields*, vol. 14, pp. 49–68, 2001.
- [19] R. Cools and P. Rabinowitz, "Monomial cubature rules since "Stroud": A compilation," *J. Comput. Appl. Math.*, vol. 48, pp. 309–326, 1993.
- [20] M. M. Bibby and A. F. Peterson, "High accuracy calculation of the magnetic vector potential on surfaces," *Aces J.*, vol. 18, no. 1, pp. 12–22B, March 2003.
- [21] M. A. Khayat and D. R. Wilton, "Numerical evaluation of singular and near singular potential integrals," *IEEE Trans. Antennas Propag.*, vol. 53, no. 10, pp. 3180–3190, Oct. 2005.
- [22] T. Ozdemir and J. L. Volakis, "Triangular prisms for edge-based vector finite element analysis of conformal antennas," *IEEE Trans. Antennas Propag.*, vol. 45, no. 5, pp. 788–797, May 1997.
- [23] M. E. Honnor, J. Trevelyan, P. Bettess, M. El-hachemi, O. Hassan, K. Morgan, and J. J. Shirron, "An integration scheme for electromagnetic scattering using plane wave edge elements," *Adv. Eng. Softw.*, pp. 58–65, 2008.
- [24] E. M. Klopff, N. J. Sekeljic, M. M. Ilic, and B. M. Notaros, "Investigations of optimal geometrical and field/current modeling parameters for higher order FEM, MoM, and hybrid CEM techniques," in *Proc. USNC-URSI Nat. Radio Science Meeting*, Boulder, CO, Jan. 5–8, 2011, pp. B5–1.
- [25] B. M. Kent, "Comparative measurements of precision radar cross section (RCS) calibration targets," in *Proc. 2001 IEEE Antennas Propag. Soc. Int. Symp.*, 2001, vol. 4, pp. 412–415.
- [26] J. Ruoskanen, P. Eskelinen, H. Heikkilä, P. Kuosmanen, and T. Kiuru, "A practical millimeter-wave radar calibration target," *IEEE Antennas Propag. Mag.*, vol. 46, no. 2, pp. 94–97, Apr. 2004.
- [27] P. S. P. Wei, A. W. Reed, C. N. Ericksen, and R. K. Schuessler, "Measurements and calibrations of larger squat cylinders," *IEEE Antennas Propag. Mag.*, vol. 51, no. 2, pp. 205–212, Apr. 2009.
- [28] A. C. Woo, H. T. G. Wang, M. J. Schuh, and M. L. Sanders, "Benchmark radar targets for the validation of computational electromagnetics programs," *IEEE Antennas Propag. Mag.*, vol. 35, no. 1, pp. 84–89, Feb. 1993.
- [29] A. Yaghjian and R. McGahan, "Broadside radar cross section of the perfectly conducting cube," *IEEE Trans. Antennas Propag.*, vol. 33, pp. 321–329, Mar. 1985.
- [30] [Online]. Available: [www.feko.info/applications/white-papers/rcs-benchmarking-of-generic-shapes/](http://www.feko.info/applications/white-papers/rcs-benchmarking-of-generic-shapes/)
- [31] B. Kolundzija, V. Petrovic, A. Djordjevic, and T. Sarkar, "Efficient method of moment analysis based on imaging and edging," in *Proc. 2000 IEEE Antennas Propag. Soc. Int. Symp.*, 2000, vol. 4, pp. 2298–2301.



**Eve M. Klopff** (S'04) was born in New Orleans, LA, in 1979. She received the B.S. degree in electrical engineering from Texas A&M University, Corpus Christi, in 2002 and the M.S. degree in electrical engineering from Colorado State University, Fort Collins, in 2008.

From 2008 to 2011, she was a Research Assistant in Electromagnetics Laboratory, Department of Electrical and Computer Engineering, at Colorado State University, where she defended her Ph.D. dissertation in September 2011 and is in her final semester as a Ph.D. student. She is currently an Adjunct Instructor in the Electrical Engineering and Renewable Energy Department at the Oregon Institute of Technology. Her research interests include microwave systems and computational electromagnetics.



**Nada J. Šekeljić** (S'11) was born in Belgrade, Serbia, in 1984. She received the Dipl. Ing. (B.Sc.) degree in electrical engineering from the University of Belgrade, Serbia, in 2008.

Since 2008, she has been a Research Assistant in Electromagnetics Laboratory and Teaching Assistant in the Department of Electrical and Computer Engineering, at Colorado State University, Fort Collins, where she is working toward her Ph.D. degree. Her research interests are in computational and applied electromagnetics.



**Milan M. Ilić** (S'00–M'04) was born in Belgrade, Serbia, in 1970. He received the Dipl. Ing. and M.S. degrees in electrical engineering from the University of Belgrade, Serbia, in 1995 and 2000, respectively, and the Ph.D. degree from the University of Massachusetts, Dartmouth, in 2003.

He is currently an Associate Professor in the School of Electrical Engineering at the University of Belgrade and a postdoctoral Research Associate and Affiliated Faculty with the ECE Department of the Colorado State University. His research interests

include computational electromagnetics, antennas, and microwave components and circuits.

Dr. Ilić serves as Technical Program Committee Chair for the 11th International Workshop on Finite Elements for Microwave Engineering-FEM2012, June 4–6, 2012, Estes Park, CO. He was the recipient of the 2005 IEEE MTT-S Microwave Prize.



**Branislav M. Notaroš** (M'00–SM'03) was born in Zrenjanin, Yugoslavia, in 1965. He received the Dipl. Ing. (B.S.), M.S., and Ph.D. degrees in electrical engineering from the University of Belgrade, Belgrade, Yugoslavia, in 1988, 1992, and 1995, respectively.

From 1996 to 1999, he was an Assistant Professor in the School of Electrical Engineering at the University of Belgrade. He spent the 1998–1999 academic year as a Visiting Scholar at the University of Colorado at Boulder. He was an Assistant Professor, from 1999 to 2004, and Associate Professor, from

2004 to 2006, in the Department of Electrical and Computer Engineering at the University of Massachusetts Dartmouth. He is currently an Associate Professor of electrical and computer engineering and Director of Electromagnetics Laboratory at Colorado State University. His research interests and activities are in computational electromagnetics, antennas, and microwaves, and in particular in higher order computational electromagnetic techniques based on the method of moments, finite element method, physical optics, domain decomposition method, diakoptics, and hybrid methods as applied to modeling and design of antennas, scatterers, and microwave circuits and devices. His publications include about 90 journal and conference papers, and three workbooks in electromagnetics and in fundamentals of electrical engineering (basic circuits and fields). He is the author of a textbook *Electromagnetics* (Prentice-Hall, 2010) for undergraduates as well as the Electromagnetics Concept Inventory (EMCI), an assessment tool for electromagnetic fields and waves.

Dr. Notaroš serves as General Chair for the 11th International Workshop on Finite Elements for Microwave Engineering-FEM2012, June 4–6, 2012, Estes Park, Colorado, USA. He was the recipient of the 2005 IEEE MTT-S Microwave Prize (best-paper award for IEEE Transactions on MTT), 1999 IEE Marconi Premium (best-paper award for IEE Proceedings on Microwaves, Antennas and Propagation), 1999 URSI Young Scientist Award, 2005 UMass Dartmouth Scholar of the Year Award, 2004 UMass Dartmouth College of Engineering Dean's Recognition Award, 1992 Belgrade Chamber of Industry and Commerce Best M.S. Thesis Award, 2009, 2010, and 2011 Colorado State University Electrical and Computer Engineering Excellence in Teaching Awards, 2010 Colorado State University College of Engineering George T. Abell Outstanding Teaching and Service Faculty Award, and 2012 Colorado State University System Board of Governors Excellence in Undergraduate Teaching Award.